Published in final edited form as:
Sens Actuators B Chem. 2014 February 1; 191: . doi:10.1016/j.snb.2013.10.008.

Microfluidic Valves Made From Polymerized Polyethylene Glycol Diacrylate

Chad I. Rogers[†], **Joseph B. Oxborrow**[‡], **Ryan R. Anderson**[‡], **Long-Fang Tsai**[‡], **Gregory P. Nordin**[‡], and **Adam T. Woolley**[†,*]

[†]Department of Chemistry and Biochemistry, Brigham Young University, Provo, UT 84602

[‡]Department of Electrical and Computer Engineering, Brigham Young University, Provo, Utah 84602

Abstract

Pneumatically actuated, non-elastomeric membrane valves fabricated from polymerized polyethylene glycol diacrylate (poly-PEGDA) have been characterized for temporal response, valve closure, and long-term durability. A ~100 ms valve opening time and a ~20 ms closure time offer valve operation as fast as 8 Hz with potential for further improvement. Comparison of circular and rectangular valve geometries indicates that the surface area for membrane interaction in the valve region is important for valve performance. After initial fabrication, the fluid pressure required to open a closed circular valve is ~50 kPa higher than the control pressure holding the valve closed. However, after ~1000 actuations to reconfigure polymer chains and increase elasticity in the membrane, the fluid pressure required to open a valve becomes the same as the control pressure holding the valve closed. After these initial conditioning actuations, poly-PEGDA valves show considerable robustness with no change in effective operation after 115,000 actuations. Such valves constructed from non-adsorptive poly-PEGDA could also find use as pumps, for application in small volume assays interfaced with biosensors or impedance detection, for example.

Keywords

membrane valve; non-adsorptive polymer; non-elastomeric polymer; pneumatic actuation; poly-PEGDA; valve characterization; valve response

1. Introduction

Microfluidics is an expanding and vibrant field of research that spans multiple scientific disciplines, including physics, engineering, chemistry, biology, and medicine [1–3]. Areas of emphasis range from materials development [1, 4] and device fabrication [5, 6] to biosensing [7, 8] and point-of-care diagnostics [9, 10]. Some advantages of microfluidics are small sample and reagent volumes, potential for mass production to create low-cost devices, reduced distance for diffusion, high surface-to-volume ratios, and the ability to integrate multiple processes in a single device [1].

[*]To whom correspondence should be addressed. Phone: 801-422-1701. atw@byu.edu.

An important facet of microfluidic systems is the need to control the movement of fluid. Many methods have been used to control liquids in microdevices including voltage [11, 12], valves [13–15], and channel geometry [16, 17]. Active valves are particularly promising for fluid manipulation due to the ability to rapidly switch between open and closed positions [10]. Microfabricated valves first introduced by Unger et al. [14] were fabricated using two embedded channels in polydimethylsiloxane (PDMS). When pressure was applied to the upper control channel, the flexible PDMS between the channels collapsed into the lower channel and closed it; the valve reopened when the control pressure was released. Later, Grover et al. [15] demonstrated a ~250 μm thick membrane valve that consisted of a middle PDMS elastomeric layer sandwiched between two rigid glass layers. Flow through the valve was prevented when pressure was applied to the membrane, pushing it against a pedestal within the fluid channel (e.g., blue inset, Figure 1A). The valve was opened with an applied vacuum to lift the membrane off the pedestal. Membrane valves can also be used in pumps [18, 19]. A key focus of current microfluidics research is integration of multiple processes (e.g., sample preparation, separation, and detection) to provide a complete sample analysis package, requiring minimal user intervention. Microfabricated valves find use in integrated devices ranging from automated systems, such as those where valves are utilized to control and direct fluid for small molecule analysis in the search for life on Mars [20], to physiological mimicry, such as in a microvasculatory microchip system [21].

Ideally, valves should have a small volume (< 1 nL), be non-adsorptive, resist swelling, and be easily fabricated. PDMS is a common valve material because it is easy to mold; however, it is prone to nonspecific adsorption of proteins and permeation of hydrophobic molecules [22], which is problematic for bioanalytical applications and nonideal for valves. In response to this disadvantage, other materials (fluoroelastomers [23–25] and thermoplastic elastomer [26]) have been explored as valve membranes in conjunction with rigid fluidic substrates of cyclic olefin copolymer, poly(methyl methacrylate), or glass. Fluoroelastomers, while resistant to nonspecific adsorption, are normally opaque and difficult to bond. Thermoplastic elastomers, although an improvement over PDMS, are still prone to nonspecific adsorption without chemical modification [27]. Polycarbonate, a non-elastomeric polymer, has been used as a valve membrane in a genetic sensor for tuberculosis; in this setup a solenoid mechanically forced the valve closed [28]. More recently, Chen et al. [29] demonstrated a pneumatically actuated polystyrene valve for oral fluid analysis. However, polycarbonate and polystyrene are both prone to nonspecific adsorption, and require large valve areas (>3 mm^2) that lead to greater dead volumes that limit device miniaturization. Polymerized polyethylene glycol diacrylate (poly-PEGDA), another non-elastomeric polymer, is innately resistant to nonspecific adsorption and small molecule permeation [22]. Although this polymer has a higher elastic modulus (>0.1 GPa) [30, 31] than elastomers, its non-adsorptive nature makes it attractive as a material for monolithic membrane valves.

Here we demonstrate for the first time the construction of all-poly-PEGDA membrane valves for microfluidics. These valves have an 8x smaller area footprint (0.38 mm^2) than previously demonstrated non-elastomeric (and typically adsorptive) membrane valves. Our valves are actuated via standard pressurized control, but do not require an elastomeric membrane material. We have evaluated several different valve designs, including rectangular and circular geometries. Moreover, we have characterized the temporal response and flow performance of these poly-PEGDA valves over a range of pressures and number of actuations.

2. Materials and methods

2.1. Reagents and materials

Azobisisobutyronitrile (AIBN), polyethylene glycol diacrylate (PEGDA, M.W. 258), and 2,2′-dimethoxy-2-phenylacetophenone (DMPA) were purchased from Sigma Aldrich (Milwaukee, WI). Phosphate buffered saline (PBS, 10x) was obtained from Fisher Scientific (Pittsburgh, PA) and diluted to 1x by adding deionized (DI) water (18.3 MΩ) from a Barnstead EASYpure UV/UF compact reagent grade water system. Perfluorosilane, (tridecafluoro-1,1,2,2-tetrahydrooctyl)-1-trichlorosilane, was purchased from UCT Specialties (Bristol, PA). SU8 photoresist (2005, 2010, 2025, and 2050) was obtained from Microchem (Newton, MA).

2.2. Device fabrication

Thermally initiated prepolymer solutions were prepared by mixing 0.01 % w/w AIBN in PEGDA. Photoinitiated prepolymer solutions were prepared by combining 0.015 % w/w DMPA with PEGDA. Solutions were vortexed for 15 s, sonicated for 15 min, and subsequently refrigerated until use.

Poly-PEGDA valves were fabricated in three general processes: thermal polymerization of control and fluidic layers, photoinitiated polymerization of the membrane layer, and final device assembly and bonding (Figure 2). The molds for thermal polymerization were formed using a clean silicon wafer (Figure 2A) on which SU8 features (~80 μm thick for the control layer and ~30 μm thick for the fluidic layer) had been photolithographically patterned (Figure 2B) [22]. The mold was placed inside a glass container containing one drop of perfluorosilane, which began to evaporate when heated to 70°C [32]. The perfluorosilane was vapor deposited onto the surface for 10 min to ease polymer removal from the mold. Poly-PEGDA spacers (~500 μm) were used to define the mold height (Figure 2C), and a 3.5″ glass wafer was used as a cover (Figure 2D). Prepolymer containing AIBN was then introduced into the cavity (Figure 2E), and the entire mold was placed into an oven at 80°C for 1–2 hr until polymerization was complete (Figure 2F). The glass cover slide was carefully removed to avoid breaking the wafer (Figure 2G), and the polymerized layers were subsequently removed, diced, and cleaned with acetone and 2-propanol (Figure 2H).

Membrane fabrication was accomplished in a similar fashion, but photopolymerization was used. A clean glass slide was placed on a silicon wafer (Figure 2A), and Mylar spacers (42 μm) were used to define the mold height (Figure 2C). A glass slide was placed on top (Figure 2D), and 70 μL of prepolymer containing DMPA was introduced into the mold cavity (Figure 2E). UV exposure at 365 nm (560 mJ/cm^2) for 110 s was used to polymerize the membrane (Figure 2F). The top surface of the membrane was exposed by removing the glass slide (Figure 2G) immediately before bonding to the control layer (Figure 2I). A clamp was used to hold the layers in contact during two subsequent UV exposures at 365 nm: the first was at 1.84 J/cm^2 for 6 min in a Karl Suss mask aligner and the second was a 12 J/cm^2 exposure for 4 min using a Spectroline SB-100PR UV lamp. Once these layers were bonded, input/output holes were laser cut for the fluid channel, and the bonded control/membrane layer was removed from the glass slide and rinsed with 2-propanol (Figure 2J). The control/membrane layer was then aligned to the fluid channel layer and clamped together (Figure 2K). Vacuum was applied to the control/membrane layer during alignment and bonding (see Appendix A, Figure A1) to prevent the membrane from being polymerized to the pedestal during the final bonding step. A 42 J/cm^2 UV exposure for 14 min using the Spectroline UV lamp was used to bond the fluid layer and form the completed device (Figure 2L).

Several different valve geometries were explored. Rectangular valves (700 μm x 600 μm) with 5, 15, and 30 μm pedestals were fabricated, as were circular valves with a 350 μm

radius and 5, 15, 30, and 125 μm pedestal widths). The width of the fluid channels in the circular valves was 100 μm (see Figure 1); the fluid channel width in the rectangular valves expanded from 100 μm to 600 μm to match the valve dimensions. Channel depths in these devices ranged between 25–35 μm, membranes were ~40 μm thick, and the control channel height was 55–80 μm.

2.3. Device characterization setup

Three-layer poly-PEGDA devices were evaluated for functionality, response, and performance. Water contact angles were measured using a Ramé-Hart goniometer (model 100) with 10 μL water droplets. In previous work [22] we used Nanoports (Upchurch Scientific, Oak Harbor, WA) to connect external fluid lines to poly-PEGDA microfluidics. Herein, a piece of PDMS was clamped on top of a completed device, and hollow metal pins were used to connect the fluid and air lines to the device (see Figure A2 in Appendix A), similar to what has been done in some conventional PDMS microfluidic devices [33, 34]. A syringe pump with an inline pressure sensor (Honeywell 24PCFFA6G) was used to supply fluid to the valve. Regulated, pressurized air with an inline pressure sensor (Honeywell 24PCFFH6G) provided pressure to the control layer. Solenoid valves (Clippard EVO-3M-24) were used to switch control layer pressure for valve actuation. Valves were evaluated by comparing the fluid pressure required for flow to commence at a given control pressure. Video was recorded of meniscus movement in the output tubing and processed using custom LabView code to determine linear flow velocity, which was then converted to volumetric flow rate. When fluid flow through the valve was >0.02 μL/min (0.2% of the syringe pump driven 10 μL/min flow rate), the valve was considered to be open.

The Young's modulus for poly-PEGDA was determined from the pressure needed to deflect ~190 μm thick circular membranes with a 870 μm radius a distance of 20 μm (for linear deflection up to one half of the membrane thickness) using equation (1) [35], where P is the applied pressure in Pa, E is the elastic modulus in Pa, r is the membrane radius in m, h is the membrane thickness in m, ν is the Poisson's ratio (estimated to be 0.35 from data reported for poly(methyl methacrylate) or PMMA [36]), and y is the deflection (in m) at the membrane center.

$$\frac{Pr^4}{Eh^4}=\frac{16y}{3(1-v^2)h}+\frac{7-v}{3(1-v)}\left(\frac{y}{h}\right)^3 \quad (1)$$

The pressure needed to deflect thinner and smaller circular membrane valves with radii of 350 μm and thicknesses of 45 μm was also determined. We measured a range of deflection distances by using different thicknesses (5, 9, and 22 μm) of patterned SU8 spacers.

The temporal response of valves was measured using a high-speed camera (Photron FASTCAM SA3). We determined the change in grayscale intensity in the images, which was then related linearly to the percent deflection at the center of the valve during actuation. A valve actuation rate of 1 Hz with a 30% duty cycle and 200 kPa control pressure was used to evaluate the fall (closure) and rise (open) time of valves. The rise time was given by the time required for the valve position to go from 10–90% of its range of motion, and the fall time was determined from the time required for the valve position to drop from 90–10% of its motion range.

Valve performance was evaluated over a range of control pressures (0–200 kPa) and as a function of number of actuations. PBS (~250 μL) was flowed through the fluid layer of each device before evaluating valves. Control and fluid pressures were raised incrementally from lower to higher (0, 70, 150, 200 kPa). Each valve was actuated at 1 Hz and a 50% duty cycle

in increments of 500 for initial testing and larger increments (up to 100,000) for long-term testing. Each valve was retested over the same range of pressures after each series of actuations. Circular valves with both 15 and 30 μm pedestal widths were used in duty cycle tests.

3. Results and discussion

3.1. Device characterization results

Figure 1 shows an overview of monolithic membrane valves fabricated entirely from poly-PEGDA. Applied pressure is used to close the valve, preventing fluid from flowing through (Figure 1A), and the valve is opened by releasing the control pressure, and allowing fluid pressure to deflect the membrane up, resuming flow. Top-view images of the valve with green colored dye in the fluid channel demonstrate the opening and closure of a valve with a 700 μm diameter and a 30 μm pedestal (Fig. 1A-right images). The membrane is deflected up during fabrication, to prevent bonding to the valve seat (Figure 1B). An SEM image shows a cross-sectional cut through a poly-PEGDA valve (Figure 1C) demonstrating the three-layer fabrication with the deeper control layer channels on top, the poly-PEGDA membrane in the middle, and the shallower fluid channel on the bottom. Our measured water contact angle of 55° for poly-PEGDA indicates a more hydrophilic surface compared to PMMA (68°) [37] and PDMS (100°) [38].

We determined the elastic modulus for poly-PEGDA to be 0.13 ± 0.03 GPa, based on membrane deflection under applied pressure (data used in our calculations are provided in Table A1 in Appendix A). This modulus is too high for poly-PEGDA to form self-collapsible valves like ones that have been made from PDMS, which has a formula-dependent Young's modulus of 0.05–4 MPa [39]. However the elastic modulus of poly-PEGDA is acceptable for its application in membrane valves.

We characterized circular valves with 5, 15, 30, and 125 μm pedestals, and ~30 μm deep fluid channels. With these device dimensions, the 5 μm pedestals became damaged during fabrication such that functional devices were difficult to achieve. However, valves with pedestal widths of 15, 30, and 125 μm all demonstrated similar properties and function. Since valves with larger pedestals (>100 μm) occupy more device space, we focused on characterizing circular valves with 15 μm and 30 μm pedestals. Rectangular valves (see Appendix A, Figure A3) were also characterized but did not maintain a linear relationship between the control pressure and fluid pressure to initiate flow, unlike circular valves. A summary of results for the various valve parameters tested is presented in Table 1.

The temporal response of circular valves demonstrated rapid and repeatable actuation (Figure 3). A fall time of 0.019 s to close the valve was determined from the time for the membrane to move from 90% deflected to 10% deflected upon switching on the control pressure. The time required to open the valve after switching off the control pressure (rise time) was 0.105 s. We used the smoothed data in this calculation due to minor noise in the position measurement as it approached 90% deflection. These rise and fall times are sufficiently rapid for utilization in microfluidic systems for actuation rates up to 8 Hz. Faster opening times could likely be achieved with either backpressure on the pumped fluid or the application of vacuum to the valve in the opening step.

Valves were evaluated by monitoring fluid pressure and flow for a given control pressure. In Figure 4, a circular valve with a 30 μm pedestal was tested after the valve had been actuated ~5,000 times. The control pressure was held constant at 97 kPa, and after 30 s fluid was pressurized into the valve by a syringe pump at 10 μL/min. The 30 s delay in the syringe pump activation provided a baseline for the fluid pressure. Once flow was initiated, the fluid

pressure increased until it exceeded the control pressure, at which point the valve opened, providing an outlet for the pressure and resulting in flow that rapidly increased towards the pump rate. Monitoring of fluid and control pressures as well as meniscus movement, was used in evaluating >40 different valves, all of which demonstrated similar behavior. Similar tests were done multiple times for each valve geometry and pedestal width across a range of pressures and a number of valve actuations. In conjunction with the experimental data, we also calculated the membrane deflection as a function of applied pressure using equation (2), which is a rearrangement of equation (1) with the other variables set equal to P:

$$P=\frac{Ehy\left((v^2-6v-7)y^2-16h^2\right)}{3r^4(v^2-1)} \quad (2)$$

In Figure 5 we plot this pressure versus membrane deflection relationship for a typical microvalve design, with a 45 μm thick circular membrane having a 350 μm radius, an elastic modulus of 0.13 GPa, and a Poisson's ratio of 0.35. Figure 5 also shows experimental deflection results for poly-PEGDA membranes having the same thickness and radius as for the calculated curve, and the experimental data agree well with the calculated result. These experimentally measured deflections show a similar trend to the calculated data, with increasing pressure (17, 30, and 111 kPa) required to deflect a membrane over greater distances (5, 9, and 22 μm, respectively). Importantly, only a <9 kPa difference in pressure is needed for the membrane to deflect >2 μm, which is more than sufficient for flow. This result agrees very well with the experimental data in Figure 4: when the fluid pressure is less than the control pressure, no flow is observed up to 95 kPa (~98% of the 97 kPa control pressure). Flow then rapidly increases from ~0.02 μL/min to >10 μL/min as the fluid pressure is raised by 10 kPa to 105 kPa, in excellent correlation with our calculation.

The relationship between the control pressure and the fluid pressure at which flow commenced was determined in multiple devices and after various numbers of actuations. Valves were expected to open once the fluid pressure exceeded the applied control pressure. However, for newly fabricated devices a ~50 kPa excess fluid pressure was required to initiate flow through valves (Figure 6A). One possible explanation of this initial pressure offset is stiction between the membrane and the pedestal. However, there was no clear trend in initial pressure offset as pedestal width varied from 15–125 μm. When the valve was actuated 500–1500 times, the fluid pressure required to open the valve decreased toward the control pressure until the plot of fluid vs. control pressure reached a slope of 1 after 1000–1500 actuations. Realignment of polymer chains in the device after multiple valve actuations [40] could increase the elasticity of the membrane, thereby making it easier to close. We have further evaluated valves for long-term robustness after very large numbers of actuations (Figure 6B). After 5,000, 15,000, and even 115,000 actuations, the fluid vs. control pressure plot maintained a linear relationship with a slope of 1, thus demonstrating considerable repeatability and potential for long-term use. Since 1000–1500 actuations were needed for valves to show the expected fluid vs. control pressure relationship, we preconditioned our valves by performing 1500 actuations before use.

Several different valve designs were evaluated (see summary in Table 1). Rectangular valves with 5, 15, and 30 μm pedestals were tested. As with circular valves, rectangular valves with 5 μm pedestals were easily damaged during fabrication. Unlike in circular valves (Figure 1), the fluid channel was widened in rectangular valves to match the control layer design (Appendix A, Figure A3). Rectangular valves did not follow the linear fluid vs. control pressure relationship observed for circular valves in Figure 6B. In addition, the rectangular valve designs were not as effective as circular ones in valve closure at low control pressures (<70 kPa). The better performance of the circular valves is likely due to

the larger surface area of the valve seat in contact with the membrane, which helps the membrane to remain planar in the closed state. In contrast, the valve seat contact area with the membrane is limited to the pedestal only in the rectangular valve design, so the membrane may deflect partially into the fluid layer. Valves remained functional, without irreversible membrane deformation, for fluid pressures up to the maximum tested (400 kPa) and flow up to the maximum used (150 μL/min).

3.2. Device prospects

Three-layer poly-PEGDA valves have reliable fabrication, fast response times, and robustness over a large number of actuations. Valves with pedestal widths down to 15 μm have been successfully made and operated. Possible improvements to these valves include smaller diameters (<200 μm) and fluid channel widths (<50 μm), and thinner membranes (<20 μm), all of which would further reduce dead volume and improve performance. With combined application of control pressure and vacuum to control lines and appropriate device layouts, arrays of these poly-PEGDA valves have potential for application as peristaltic pumps [18, 19]. Poly-PEGDA valve integration with functional or sensing components in other materials, such as silicon or glass, is also attractive. Finally, the fabrication of embedded electrodes into devices would enable conductivity or impedance detection, as well as valve closure determination.

Poly-PEGDA valves with their intrinsic resistance to nonspecific adsorption are ideally suited for biomolecular and protein assays. One example would be the analysis of Tau protein in cerebrospinal fluid for brain trauma diagnosis [41, 42] via an on-chip microdialysis system [43] that extracts small volumes of cerebrospinal fluid, which could then be fluorescently labeled and purified on-chip [44] for subsequent electrophoretic separation and detection. Similarly, thymidine kinase I in blood serum, which shows promise in diagnosis of hematological cancers [45], could be captured on-chip using immobilized antibodies [46], and then reacted with a fluorescently labeled secondary antibody for detection using laser induced fluorescence [47]. A final example is the quantitative analysis of pre-term birth biomarkers in blood serum [48, 49], utilizing poly-PEGDA valves to control sample introduction and pumping for secondary flow required for nanospray mass spectrometry [50]. In these examples, a non-adsorptive device material would enable more of the analyte of interest to be available for detection and provide symmetrical separation peaks.

4. Conclusions

Poly-PEGDA with inherent nonspecific adhesion resistance properties has been used to form microfluidic valves. Multiple device geometries were tested; a circular design had a linear, slope of one, fluid versus control pressure plot over different pedestal widths. A valve opening time of ~100 ms and a closure time of ~20 ms offer valve operation as fast as 8 Hz with potential for further improvement. A number of replicate measurements after a series of actuations and over a range of pressures demonstrated the functionality and robustness of these poly-PEGDA valves.

The multi-layer fabrication method developed here for valves can be adapted for on-chip pumping, which could aid in the integration of automated on-chip sample preparation with electrophoretic separation. Such pumps could also provide a mechanism for solution mixing, or find use in a closed system where small-volume specimens could be recirculated over a sensor, improving sampling. Finally, attachment of these valve systems to silicon or glass devices could be explored to enable interfacing with micro- and nano-sensors such as microcantilevers, silicon ring resonators, nanowires, etc.

Supplementary Material

Refer to Web version on PubMed Central for supplementary material.

Acknowledgments

We are grateful to the Integrated Microfabrication Lab at Brigham Young University for access to device fabrication equipment. We also thank the National Institutes of Health (R01 EB006124) and the Telford & FrankWoolley and Garth L. Lee Graduate Student Research Awards from the Department of Chemistry and Biochemistry at Brigham Young University for support of this work.

References

1. Nge PN, Rogers CI, Woolley AT. Advances in Microfluidic Materials, Functions, Integration, and Applications. Chem Rev. 2013; 113:2550–83. [PubMed: 23410114]
2. Kovarik ML, Ornoff DM, Melvin AT, Dobes NC, Wang Y, Dickinson AJ, et al. Micro Total Analysis Systems: Fundamental Advances and Applications in the Laboratory, Clinic, and Field. Anal Chem. 2013; 85:451–72. [PubMed: 23140554]
3. Arora A, Simone G, Salieb-Beugelaar GB, Kim JT, Manz A. Latest Developments in Micro Total Analysis Systems. Anal Chem. 2010; 82:4830–47. [PubMed: 20462185]
4. van Midwoud PM, Janse A, Merema MT, Groothuis GMM, Verpoorte E. Comparison of Biocompatibility and Adsorption Properties of Different Plastics for Advanced Microfluidic Cell and Tissue Culture Models. Anal Chem. 2012; 84:3938–44. [PubMed: 22444457]
5. Abgrall P, Gué AM. Lab-on-chip technologies: making a microfluidic network and coupling it into a complete microsystem—a review. J Micromech Microeng. 2007; 17:R15–R49.
6. Yang, S.; DeVoe, DL. Microfluidic Diagnostics: Methods and Protocols. Humana Press; New York City, NY: 2013. Microfluidic Device Fabrication by Thermoplastic Hot-Embossing; p. 115-23.
7. Trzebinski J, Sharma S, Radomska-Botelho Moniz A, Michelakis K, Zhang Y, Cass AEG. Microfluidic device to investigate factors affecting performance in biosensors designed for transdermal applications. Lab Chip. 2012; 12:348–52. [PubMed: 22130554]
8. Rivet C, Lee H, Hirsch A, Hamilton S, Lu H. Microfluidics for medical diagnostics and biosensors. Chem Eng Sci. 2011; 66:1490–507.
9. Chin CD, Linder V, Sia SK. Commercialization of microfluidic point-of-care diagnostic devices. Lab Chip. 2012; 12:2118–34. [PubMed: 22344520]
10. Gervais L, de Rooij N, Delamarche E. Microfluidic Chips for Point-of-Care Immunodiagnostics. Adv Mater. 2011; 23:H151–76. [PubMed: 21567479]
11. Mainz ER, Gunasekara DB, Caruso G, Jensen DT, Hulvey MK, Fracassi da Silva JA, et al. Monitoring intracellular nitric oxide production using microchip electrophoresis and laser-induced fluorescence detection. Anal Methods. 2012; 4:414–20.
12. Jin S, Anderson GJ, Kennedy RT. Western Blotting Using Microchip Electrophoresis Interfaced to a Protein Capture Membrane. Anal Chem. 2013; 85:6073–9. [PubMed: 23672369]
13. Kim J, Kang M, Jensen EC, Mathies RA. Lifting Gate Polydimethylsiloxane Microvalves and Pumps for Microfluidic Control. Anal Chem. 2012; 84:2067–71. [PubMed: 22257104]
14. Unger MA, Chou HP, Thorsen T, Scherer A, Quake SR. Monolithic Microfabricated Valves and Pumps by Multilayer Soft Lithography. Science. 2000; 288:113–6. [PubMed: 10753110]
15. Grover WH, Skelley AM, Liu CN, Lagally ET, Mathies RA. Monolithic membrane valves and diaphragm pumps for practical large-scale integration into glass microfluidic devices. Sens Actuators B. 2003; 89:315–23.
16. Mohammed MI, Desmulliez MPY. The manufacturing of packaged capillary action microfluidic systems by means of CO2 laser processing. Microsyst Technol. 2013; 19:809–18.
17. Au AK, Lai H, Utela BR, Folch A. Microvalves and Micropumps for BioMEMS. Micromachines. 2011; 2:179–220.
18. Grover WH, Mathies RA. An integrated microfluidic processor for single nucleotide polymorphism-based DNA computing. Lab Chip. 2005; 5:1033–40. [PubMed: 16175257]

19. Stockton AM, Mora MF, Cable ML, Willis PA. Design rules and operational optimization for rapid, contamination-free microfluidic transfer using monolithic membrane valves. Sens Actuators B. 2013; 177:668–75.
20. Kim J, Jensen EC, Stockton AM, Mathies RA. Universal Microfluidic Automaton for Autonomous Sample Processing: Application to the Mars Organic Analyzer. Anal Chem. 2013; 85:7682–8. [PubMed: 23675832]
21. Schimek K, Busek M, Brincker S, Groth B, Hoffmann S, Lauster R, et al. Integrating biological vasculature into a multi-organ-chip microsystem. Lab Chip. 2013; 13:3588–98. [PubMed: 23743770]
22. Rogers CI, Pagaduan JV, Nordin GP, Woolley AT. Single-Monomer Formulation of Polymerized Polyethylene Glycol Diacrylate as a Nonadsorptive Material for Microfluidics. Anal Chem. 2011; 83:6418–25. [PubMed: 21728310]
23. Willis PA, Greer F, Lee MC, Smith JA, White VE, Grunthaner FJ, et al. Monolithic photolithographically patterned Fluorocur PFPE membrane valves and pumps for in situ planetary exploration. Lab Chip. 2008; 8:1024–6. [PubMed: 18584073]
24. Ogilvie IRG, Sieben VJ, Cortese B, Mowlem MC, Morgan H. Chemically resistant microfluidic valves from Viton membranes bonded to COC and PMMA. Lab Chip. 2011; 11:2455–9. [PubMed: 21617822]
25. Huang S, He Q, Chen H, Huang J. Preparation of normally open microvalves with fluorinated ethylene propylene membrane and poly(methyl methacrylate) substrates. Microfluid Nanofluid. 2013; 14:329–35.
26. Rupp J, Schmidt M, Münch S, Cavalar M, Steller U, Steigert J, et al. Rapid microarray processing using a disposable hybridization chamber with an integrated micropump. Lab Chip. 2012; 12:1384–8. [PubMed: 22361890]
27. Pan T, Fiorini GS, Chiu DT, Woolley AT. In-channel atom-transfer radical polymerization of thermoset polyester microfluidic devices for bioanalytical applications. Electrophoresis. 2007; 28:2904–11. [PubMed: 17640094]
28. Wang H, Chen HW, Hupert ML, Chen PC, Datta P, Pittman TL, et al. Fully Integrated Thermoplastic Genosensor for the Highly Sensitive Detection and Identification of Multi-Drug-Resistant Tuberculosis. Angew Chem. 2012; 124:4425–9.
29. Chen Z, Abrams WR, Geva E, de Dood CJ, González JM, Tanke HJ, et al. Development of a Generic Microfluidic Device for Simultaneous Detection of Antibodies and Nucleic Acids in Oral Fluids. BioMed Res Int. 2013; 2013:543294. [PubMed: 23509739]
30. Kim P, Jeong HE, Khademhosseini A, Suh KY. Fabrication of non-biofouling polyethylene glycol micro- and nanochannels by ultraviolet-assisted irreversible sealing. Lab Chip. 2006; 6:1432–7. [PubMed: 17066166]
31. Rogers, CI.; Pagaduan, JV.; Nordin, GP.; Woolley, AT. Utilizing Polymerized Polyethylene Glycol Diacrylate for Microfluidic Valves. Pittcon Conference and Expo; Orlando, FL. March 11–15, 2012;
32. Lee JK, Kung MC, Kung HH, Mockros LF. Microchannel technologies for artificial lungs: (3) open rectangular channels. ASAIO J. 2008; 54:390–5. [PubMed: 18645356]
33. Balagaddé FK, You L, Hansen CL, Arnold FH, Quake SR. Long-Term Monitoring of Bacteria Undergoing Programmed Population Control in a Microchemostat. Science. 2005; 309:137–40. [PubMed: 15994559]
34. Ren L, Wang JC, Liu W, Tu Q, Liu R, Wang X, et al. An enzymatic immunoassay microfluidics integrated with membrane valves for microsphere retention and reagent mixing. Biosens Bioelectron. 2012; 35:147–54. [PubMed: 22421588]
35. Kovacs, GTA. Micromachined Transducers Sourcebook. McGraw-Hill; New York: 1998. Micromachined Transducers Sourcebook; p. 250
36. Goswami A, Umarji AM, Madras G. Thermomechanical and fractographic behavior of poly (HDDA-coMMA): a study for its application in microcantilever sensors. Polym Adv Technol. 2012; 23:1604–11.
37. Ma Y, Cao X, Feng X, Ma Y, Zou H. Fabrication of super-hydrophobic film from PMMA with intrinsic water contact angle below 90°. Polymer. 2007; 48:7455–60.

38. Lawton RA, Price CR, Runge AF, Doherty WJ III, Saavedra SS. Air plasma treatment of submicron thick PDMS polymer films: effect of oxidation time and storage conditions. Colloids and Surfaces A: Physicochemical and Engineering Aspects. 2005; 253:213–5.
39. Fuard D, Tzvetkova-Chevolleau T, Decossas S, Tracqui P, Schiavone P. Optimization of poly-di-methyl-siloxane (PDMS) substrates for studying cellular adhesion and motility. Microelectron Eng. 2008; 85:1289–93.
40. McKeen, LW. The Effect of Creep and Other Time Related Factors on Plastics and Elastomers. 2. Burlington, MA: Elsevier Inc; 2009. p. 26
41. Süssmuth SD, Reiber H, Tumani H. Tau protein in cerebrospinal fluid (CSF): a blood–CSF barrier related evaluation in patients with various neurological diseases. Neurosci Lett. 2001; 300:95–8. [PubMed: 11207383]
42. Franz G, Beer R, Kampfl A, Engelhardt K, Schmutzhard E, Ulmer H, et al. Amyloid beta 1-42 and tau in cerebrospinal fluid after severe traumatic brain injury. Neurology. 2003; 60:1457–61. [PubMed: 12743231]
43. Huynh BH, Fogarty BA, Nandi P, Lunte SM. A microchip electrophoresis device with on-line microdialysis sampling and on-chip sample derivatization by naphthalene 2,3-dicarboxaldehyde/2-mercaptoethanol for amino acid and peptide analysis. J Pharm Biomed Anal. 2006; 42:529–34. [PubMed: 16829012]
44. Nge PN, Pagaduan JV, Yu M, Woolley AT. Microfluidic chips with reversed-phase monoliths for solid phase extraction and on-chip labeling. J Chromatogr A. 2012; 1261:129–35. [PubMed: 22995197]
45. Alegre MM, Robison RA, O'Neill KL. Thymidine Kinase 1: A Universal Marker for Cancer. Cancer Clin Oncol. 2013; 2:159–67.
46. Yang W, Yu M, Sun X, Woolley AT. Microdevices integrating affinity columns and capillary electrophoresis for multibiomarker analysis in human serum. Lab Chip. 2010; 10:2527–33. [PubMed: 20664867]
47. Salehi-Reyhani A, Kaplinsky J, Burgin E, Novakova M, deMello AJ, Templer RH, et al. A first step towards practical single cell proteomics: a microfluidic antibody capture chip with TIRF detection. Lab Chip. 2011; 11:1256–61. [PubMed: 21347466]
48. Vance CJ, Esplin MS, Hamblin S, Graves SW. Alterations in uterine sodium pump abundance may contribute to the onset and progression of term and preterm labor in mice. Am J Obstet Gynecol. 2006; 195:1407–14. [PubMed: 16875653]
49. Esplin MS, Merrell K, Goldenberg R, Lai Y, Iams JD, Mercer B, et al. Proteomic identification of serum peptides predicting subsequent spontaneous preterm birth. Am J Obstet Gynecol. 2011; 204:391.e1–e8. [PubMed: 21074133]
50. Chambers AG, Mellors JS, Henley WH, Ramsey JM. Monolithic Integration of Two-Dimensional Liquid Chromatography–Capillary Electrophoresis and Electrospray Ionization on a Microfluidic Device. Anal Chem. 2011; 83:842–9. [PubMed: 21214194]

Biographies

Chad Rogers graduated with his B.S. degree from the Department of Chemistry, University of Utah in 2006. He is currently a Ph.D. candidate at Brigham Young University (BYU) focusing on polymerized polyethylene glycol diacrylate microfluidics.

Joseph Oxborrow graduated with his B.S. degree in Electrical Engineering from BYU in 2011. He is pursuing a M.S. degree in Electrical Engineering at BYU.

Ryan Anderson graduated with his B.S. degree from the Department of Physics and Astronomy, BYU in 2002. He also completed his Ph.D. from the Department of Electrical and Computer Engineering, BYU in 2012 with an emphasis on the development of large microcantilever array lab-on-a-chip sensor platforms.

Long-Fang Tsai is currently a PhD candidate at BYU focusing on micro- and nanofabricated devices for microfluidics, biosensing, and MEMS.

Gregory Nordin received a B.S. degree in Physics from BYU in 1984, an M.S. in Physics from UCLA in 1986, and a Ph.D. in Electrical Engineering from the University of Southern California in 1992. From 1984 to 1992 he also worked at the Hughes Aircraft Company, the last three years of which were at the Hughes Research Laboratories in Malibu, California. From 1992 to 2005 he was in the Electrical and Computer Engineering Department at the University of Alabama in Hunstville where he was founding director of the university's Nano and Micro Devices Center. In 2005 Dr. Nordin joined BYU as Professor in the Electrical and Computer Engineering Department. His research focuses on micro- and nano-fabricated devices for biosensing, microfluidics, photonics, and MEMS.

Adam Woolley graduated with a B.S. in Chemistry from BYU in 1992. He received his Ph.D. in Chemistry in 1997 from the University of California–Berkeley and was a postdoctoral fellow at Harvard University. In 2000, Woolley joined the Department of Chemistry and Biochemistry at BYU, where he is currently a Professor and Associate Department Chair. His present research is directed toward three areas: the creation of novel and sophisticated integrated microfluidic systems for enhanced biomarker quantitation, the design of simple miniaturized biomolecular assays, and biotemplated nanofabrication.

Highlights

- We formed microfluidic valves in polymerized polyethylene glycol diacrylate.
- The polymer material for the valves is non-elastomeric and non-adsorptive.
- The performance of various valve designs was characterized.
- These valves operated reproducibly, even after over 100,000 actuations.

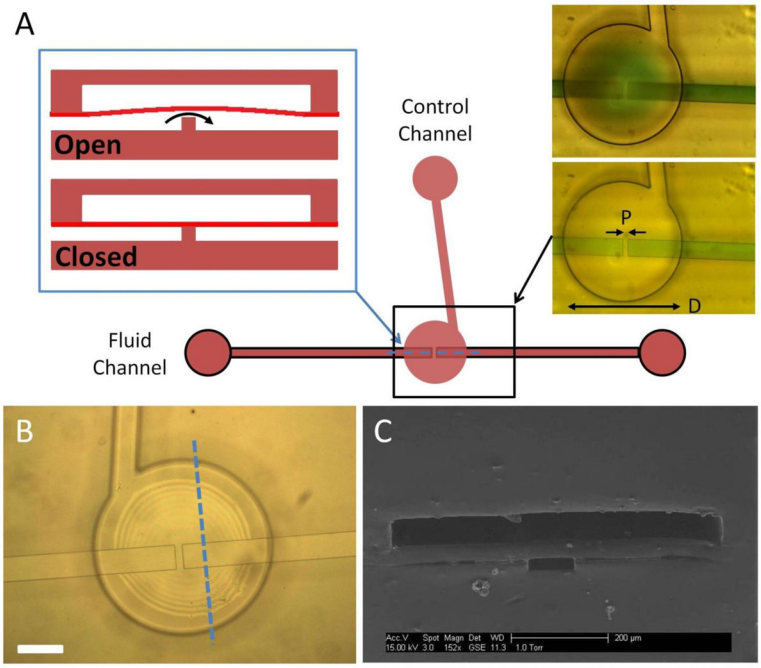

Figure 1.

Schematic of a three-layer poly-PEGDA valve. (A) The left blue inset is a cross sectional view along the dashed blue line for an open or closed valve. Top-view images on the right show an open (top) and closed (bottom) valve with green dyed fluid added for contrast. Valve diameter (D) is 700 μm, pedestal width (P) is 30 μm, and the fluid channel width is 100 μm. (B) Top-view photomicrograph of a valve before filling with liquid. Interference fringes indicate that the membrane is deflected upward after the final bonding step. White scale bar is 200 μm. (C) SEM of a three-layer valve device cross-section along the dashed blue line in (B).

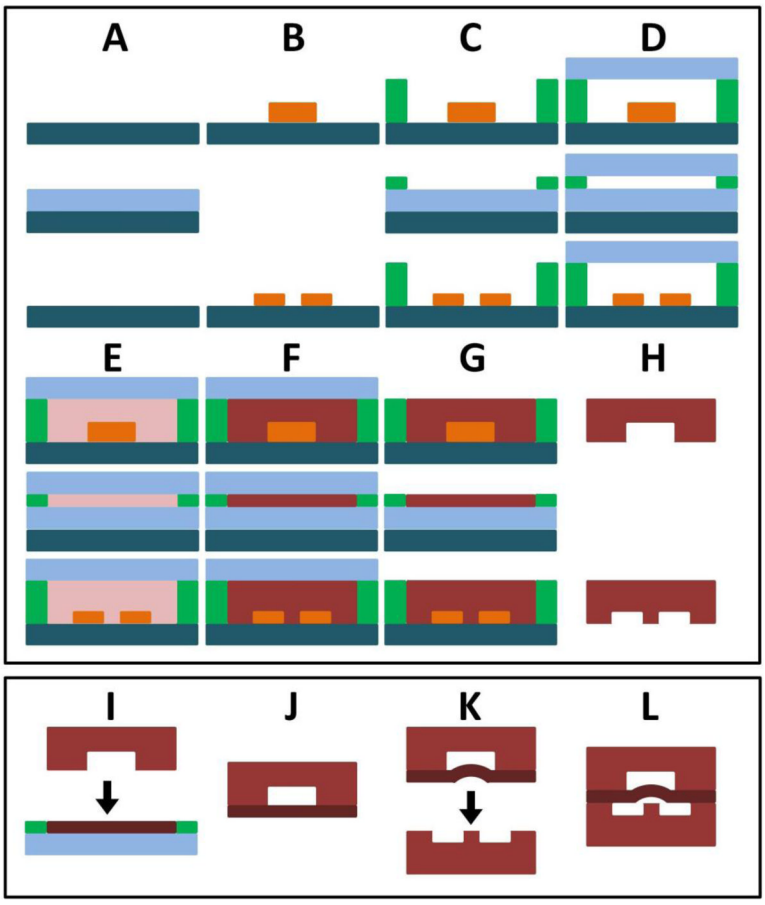

Figure 2.
Overview of poly-PEGDA valve fabrication. The top box demonstrates fabrication of the polymerized control (top), membrane (middle), and fluidic (bottom) layers. Final assembly is shown in the bottom box. (A) Clean silicon wafers. (B) SU8 patterns define features. (C) Spacers define poly-PEGDA thickness. (D) Glass wafer forms top of mold. (E) Prepolymer is introduced. (F) Polymerization of poly-PEGDA. (G) Glass cover wafer is removed. (H) Finished poly-PEGDA is removed, diced, and cleaned; an input hole is cut into the control layer. (I) The just-released top surface of the membrane layer (G, middle) is bonded to the control layer (H, top). (J) The bonded control and membrane layers are removed and (K) bonded under vacuum to the fluidic layer using UV light, (L) resulting in a completed valve device.

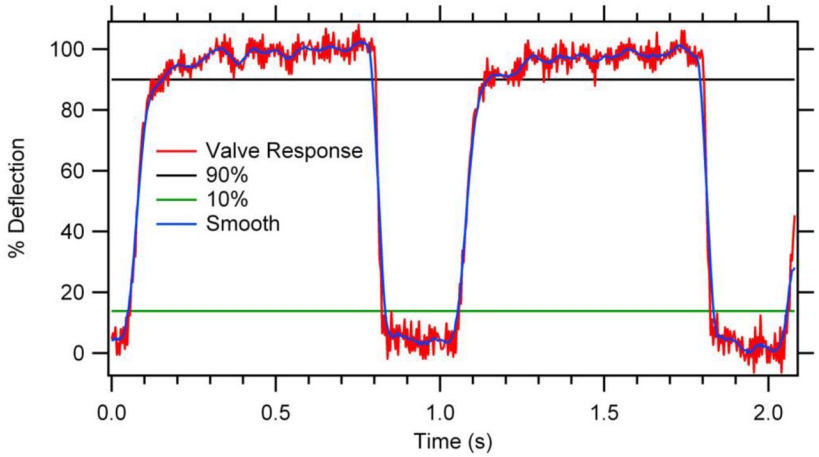

Figure 3.

Valve temporal response. Valve was actuated at 1 Hz and 30% duty cycle. Fall time (valve closure) was 0.019 s and rise time (valve opening) was 0.105 s. No vacuum was used to open the valve, and the fluid backpressure was negligible in these experiments.

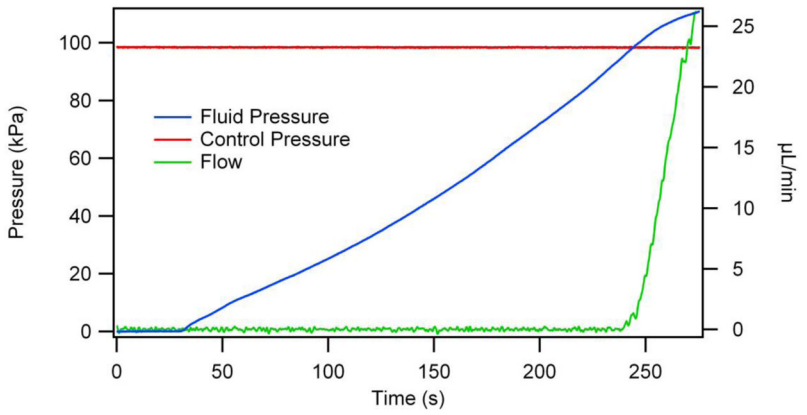

Figure 4.

Fluid pressure and volumetric flow rate as a function of time for a constant control pressure. Sensors in the fluid and control lines monitor pressures, and meniscus tracking on the fluid output allows for flow measurement. The flow rate increases rapidly once the fluid pressure exceeds the control pressure at ~240 s.

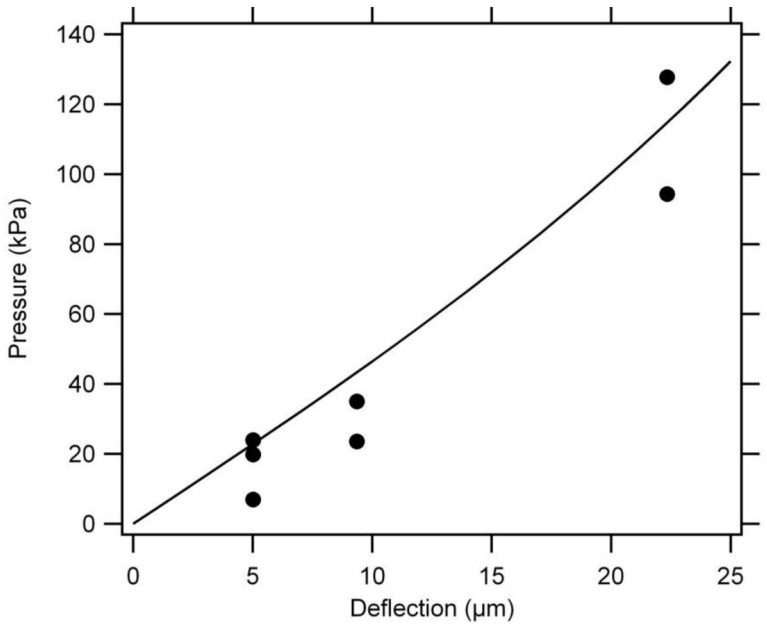

Figure 5.
Calculated (line) and experimentally measured (circles) deflection via applied pressure, for a 45 μm thick circular membrane with an elastic modulus of 0.13 GPa, a 350 μm radius, and a Poisson's ratio of 0.35. Calculated data are from Equation 2. Very low pressure (~9 kPa) is required for significant membrane deflection (>2 μm).

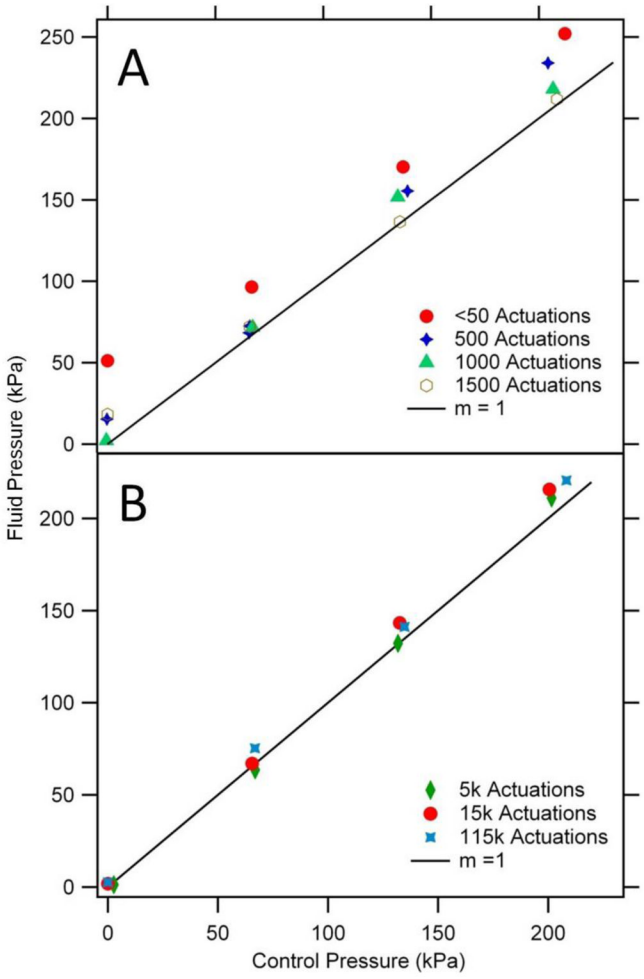

Figure 6.

Valve performance after a number of actuations as a function of control pressure. (A) Initial valve testing shows a higher fluid pressure is required to open the valve for a given control pressure. After ~1500 actuations, the fluid pressure to open a valve decreases to match the control pressure. A circular valve with a 15 μm pedestal width was used for this test. (B) Valves maintain this linear fluid vs. control pressure relationship to at least 115,000 actuations. A different circular valve with a 30 μm pedestal width was used for this test.

Table 1

Summary of results for each valve geometry.

	Circular Valve	**Square Valve**
5 μm	*Pedestals broke*	*Pedestals broke*
15 μm	*Functional valves*	*Valves leaked*
30 μm	*Functional valves*	*Valves leaked*
125 μm	*Functional valves*	*Not tested*